The ISME Journal (2015) 9, 2139–2152

www.nature.com/ismej

ORIGINAL ARTICLE

Expression profiling of the bloom-forming cyanobacterium *Nodularia* CCY9414 under light and oxidative stress conditions

Matthias Kopf[1], Fred Möke[2], Hermann Bauwe[2], Wolfgang R Hess[1] and Martin Hagemann[2]
[1]*Albert-Ludwigs-Universität Freiburg, Fakultät für Biologie, Genetik und Experimentelle Bioinformatik, Freiburg, Germany and* [2]*Universität Rostock, Institut für Biowissenschaften, Pflanzenphysiologie, Rostock, Germany*

Massive blooms of toxic cyanobacteria frequently occur in the central Baltic Sea during the summer. In the surface scum, cyanobacterial cells are exposed to high light (HL) intensity, high oxygen partial pressure and other stresses. To mimic these conditions, cultures of *Nodularia spumigena* CCY9414, which is a strain isolated from a cyanobacterial summer bloom in the Baltic Sea, were incubated at a HL intensity of 1200 μmol photons $m^{-2} s^{-1}$ or a combination of HL and increased oxygen partial pressure. Using differential RNA sequencing, we compared the global primary transcriptomes of control and stressed cells. The combination of oxidative and light stresses induced the expression of twofold more genes compared with HL stress alone. In addition to the induction of known stress-responsive genes, such as *psbA*, *ocp* and *sodB*, *Nodularia* cells activated the expression of genes coding for many previously unknown light- and oxidative stress-related proteins. In addition, the expression of non-protein-coding RNAs was found to be stimulated by these stresses. Among them was an antisense RNA to the phycocyanin-encoding mRNA *cpcBAC* and the *trans*-encoded regulator of photosystem I, PsrR1. The large genome capacity allowed *Nodularia* to harbor more copies of stress-relevant genes such as *psbA* and small chlorophyll-binding protein genes, combined with the coordinated induction of these and many additional genes for stress acclimation. Our data provide a first insight on how *N. spumigena* became adapted to conditions relevant for a cyanobacterial bloom in the Baltic Sea.
The ISME Journal (2015) **9,** 2139–2152; doi:10.1038/ismej.2015.16; published online 17 February 2015

Introduction

Cyanobacteria have an important role as primary producers in the global carbon cycle. In the central oceans, picoplanktonic cyanobacteria of the genera *Synechococcus* and *Prochlorococcus* represent the main carbon fixers (Scanlan *et al.*, 2009). In addition, cyanobacterial species capable of fixing atmospheric N_2 contribute substantial amounts of combined nitrogen to the marine food web (Zehr, 2011). Cyanobacteria also represent an important part of the phytoplankton communities in coastal, brackish and freshwater ecosystems. Many of these cyanobacteria can also produce bioactive compounds, which may have allelopathic activities against other phytoplankton organisms (Paz-Yepes *et al.*, 2013) and often exhibit toxic effects on animals, including humans (Pearson *et al.*, 2010). Mass developments ('blooms') of toxic cyanobacteria in coastal waters or freshwater systems have a dramatic impact on the use of these water bodies for recreational or drinking water purposes. It has been predicted that the expected future increases in global temperatures and atmospheric CO_2 concentrations will lead to the even further stimulation of toxic cyanobacterial blooms (Paerl and Huisman, 2008; Gehringer and Wannicke, 2014).

The Baltic Sea represents a brackish water ecosystem. Massive blooms of toxic cyanobacteria occur in its central regions almost every summer. These blooms are often dominated by *N. spumigena*, which is a filamentous cyanobacterium that produces a cocktail of bioactive compounds including the hepatotoxin nodularin (Fewer *et al.*, 2013; Mazur-Marzec *et al.*, 2013). *N. spumigena* is capable of N_2 fixation in specialized cells that are termed heterocysts (Sivonen *et al.*, 2007; Ploug *et al.*, 2011). However, the molecular basis for bloom formation is not completely understood. It is thought that excess phosphorus combined with very low nitrogen concentrations favor the growth and bloom formation of N_2-fixing cyanobacteria during the summer season (Sellner, 1997). This phenomenon particularly occurs under stably stratified warm water conditions. Then, gas vesicles that provide buoyancy to *N. spumigena*

Correspondence: M Hagemann, Universität Rostock, Institut für Biowissenschaften, Pflanzenphysiologie, Albert-Einstein-Strasse 3, Rostock D-18051, Germany.
E-Mail: martin.hagemann@uni-rostock.de
Received 31 December 2014; accepted 8 January 2015; published online 17 February 2015

and related cyanobacteria lead to the formation of large surface scums in the absence of mixing.

Hence, *Nodularia* seems to have a selective advantage in the virtually nitrogen-free conditions of the Baltic Sea, which occur during the summer as a diazotrophic cyanobacterium that has adapted to brackish waters (Möke *et al.*, 2013). The cyanobacterial filaments in the surface layer are exposed to extreme environmental conditions, such as high light (HL), high oxygen partial pressure and low nutrients, including iron and CO_2. The acclimation of cyanobacteria to such conditions can be analyzed by transcriptomic techniques. Gene expression changes under HL and oxidative stress have been reported for unicellular, non-diazotrophic model cyanobacteria, such as *Synechocystis* sp. PCC 6803 (from here: *Synechocystis*) and *Synechococcus* sp. PCC 7002 (Hihara *et al.*, 2001; Los *et al.*, 2008; Ludwig and Bryant, 2012; Kopf *et al.*, 2014), but not for representatives of bloom-forming marine strains. Recently, small non-protein-coding RNAs (ncRNAs) have been identified in cyanobacteria that are also regulated by environmental factors (Sakurai *et al.*, 2012; Georg *et al.*, 2014).

Investigations with model cyanobacteria showed that the D1 protein of photosystem 2 (PS2) represents the prime target for inactivation via HL-induced oxidative stress. In almost all cyanobacteria, the D1 protein is encoded by a small gene family that comprises D1 protein forms that are preferentially used under different light and oxygen stress conditions (reviewed by Mulo *et al.*, 2012). Moreover, a multitude of protective measures interact to prevent extensive PS2 damage. These strategies include the non-photochemical quenching achieved via the orange carotenoid protein (Kirilovsky and Kerfeld, 2012), the protective actions of special flavodiiron proteins (Allahverdiyeva *et al.*, 2013) and the activation of photorespiration under very low CO_2 and high O_2 partial pressure (Hackenberg *et al.*, 2009; Allahverdiyeva *et al.*, 2011).

In general, longer exposure to combined HL and oxidative stress is very unfavorable for oxygenic phototrophs and can only be tolerated by specialized organisms, such as bloom-forming cyanobacteria. Only recently, the first nearly complete genome sequence (Genbank accession number CP007203) of a cyanobacterium isolated from a Baltic Sea summer bloom has become available (Voß *et al.*, 2013). These data serve as a foundation for molecular studies of bloom formation using *N. spumigena* strain CCY9414 (hereafter referred to as *Nodularia* CCY9414) as a model. Here we applied the differential RNA sequencing approach (Sharma *et al.*, 2010), which provides comprehensive information on active transcriptional start sites. We analyzed global transcriptomic changes in *Nodularia* CCY9414 after exposure to HL and oxidative stress, which are characteristic for the situation in a surface scum, to identify specific adaptations to the bloom-forming lifestyle in the *Nodularia* CCY9414 genome. Our hypothesis was that those genes are not necessarily only expressed under these conditions in the bloom-forming cyanobacterium, but could be identified via comparison with data from *Synechocystis*, because they should not be present or differently regulated in cells of the non-blooming model cyanobacterium.

Materials and methods

Strain and culture conditions

N. spumigena strain CCY9414 was obtained from the Culture Collection Yerseke (CCY) at the Royal Netherlands Institute for Sea Research. It was isolated from surface waters of the Baltic Sea, east of the island of Bornholm (Hayes and Barker, 1997). Standard cultivation of axenic *Nodularia* CCY9414 cells was performed in cell culture bottles under N_2-fixing conditions with nitrate-free ASN III medium (Rippka *et al.*, 1979) supplemented with NaCl (the standard medium contained 12.5 g NaCl per liter of ASN III). The cultures were mixed daily and left to grow for 2 weeks under a 16/8 h light/dark cycle (40 μmol photons $m^{-2}s^{-1}$ of light) at 20 °C. Cells of the glucose-tolerant unicellular model strain *Synechocystis* sp. PCC 6803 were grown in CO_2-supplemented BG11 medium under standard conditions, as described previously (Hackenberg *et al.*, 2009).

For the stress experiments, *Nodularia* CCY9414 cells cultivated under the above mentioned standard conditions (that is, N_2-fixing cells in ASN III containing 12.5 g l^{-1} NaCl) were used, and one aliquot was collected immediately (control). The second aliquot of cells was exposed to 1 200 μmol photons $m^{-2}s^{-1}$ of HL (the light source was a Leica Pradovit P150 slide projector, Leica, Braunschweig, Germany) without gassing (HL stress). The third aliquot of cells was exposed to increased oxygen partial pressure via the streaming of air enriched with 40% oxygen (GMS 600 2CH, QCAL gas mixing unit, QCAL, Oberostendorf, Germany) through the cell suspension at the control light intensity of 40 μmol photons $m^{-2}s^{-1}$ (oxygen stress, $+O_2$). The fourth aliquot was exposed to HL conditions of 1200 μmol photons $m^{-2}s^{-1}$ and was additionally gassed by a stream of 40% oxygen (combined oxygen/HL stress, HL + O_2). Samples were collected at defined time intervals (0.5, 3 and 8 h) after the onset of the stress conditions.

Photosynthetic activity

The photosynthetic activity of *Nodularia* CCY9414 and *Synechocystis* was measured as O_2 production using Hansatech oxygen electrodes (Oxygraph, Norfolk, UK). A total of 4 ml of cell suspension containing ~3 μg of chlorophyll *a* per ml was used for measurements at 20 °C and 30 °C corresponding to the growth temperatures of *Nodularia* and *Synechocystis*, respectively. The cells were exposed for 5 min to light of defined photon flux rates (25–1400 μmol photons $m^{-2}s^{-1}$). Respiratory oxygen consumption was measured for 5 min in the dark,

in the cells exposed to the lowest light intensity. Chlorophyll *a* was extracted from 4 ml of cells with 90% acetone and quantified according to Arnon (1949). The soluble amino acid concentrations were determined as described by Hagemann *et al.* (2005).

RNA isolation and RT-PCR
Aliquots of 50 ml of cells obtained from the stress experiments were collected by quick filtration through sterile glass fiber filters (Whatman GF/F) that were immediately frozen in liquid nitrogen and stored at −80 °C. *Nodularia* CCY9414 total RNA was isolated using a Total RNA Isolation Kit for plants (Macherey-Nagel, Düren, Germany) as described previously (Voß *et al.*, 2013). Expression of the selected genes was analyzed using reverse-transcription PCR (RT-PCR). The RevertAid cDNA Synthesis Kit (MBI Fermentas, St. Leon-Rot, Germany) was used to generate cDNA from 1 μg of DNA-free RNA, using random hexamers as primers. The cDNA amounts were normalized to the constitutively expressed *rnpA* gene (ribonuclease P, NSP_30860). The PCR products were separated in 1% agarose gels and stained with ethidium bromide. The gene-specific primers are listed in Supplementary Table S1.

RNA sequencing
For transcriptome analysis, cDNA libraries were constructed (vertis Biotechnologie AG, Freising, Germany) and analyzed on an Illumina HiSeq 2000 sequencer as previously described (Mitschke *et al.*, 2011a, b). In brief, total RNA was enriched for primary transcripts by treatment with Terminator-5′-phosphate-dependent exonuclease (Epicentre, Madison, WI, USA). Then, 5′ppp-RNA was cleaved enzymatically using tobacco acid pyrophosphatase. The 'de-capped' RNA was ligated to an RNA linker and first-strand cDNA synthesis was initiated by random priming. Second-strand cDNA synthesis was primed with a biotinylated antisense 5′-Solexa primer, after which cDNA fragments were bound to streptavidin beads. The bead-bound cDNA was blunted and 3′-ligated to a Solexa adapter. The cDNA fragments were amplified by 22 cycles of PCR. For Illumina HiSeq 2000 (San Diego, CA, USA) analysis (100-bp read lengths), cDNAs in the size range of 200–500 bp were eluted from a preparative agarose gel. Similar numbers of reads were obtained for each cDNA library, 41 519 905 reads from the control cells, 38 851 231 reads from the HL-stressed cells and 39 503 192 reads from the combined HL + O_2 stress conditions. For normalization, the two stress libraries were scaled to the same library size as the control. Transcriptional start sites (TSSs) were predicted as previously described (Voß *et al.*, 2013), but with a higher read threshold of 620 normalized counts. The classification of the TSSs into gTSSs, iTSSs, aTSSs and nTSSs was carried out as previously described allowing a maximal distance of 200 nt to a downstream gene for the classification as gTSS (Mitschke *et al.*, 2011b).

For the detection of differentially expressed TSSs, the raw counts from all TSS positions were analyzed with the Analysis of Sequence Counts (ASC) approach (Wu *et al.*, 2010). Genes were considered to be differentially expressed, when a fold change >2 or <0.5 was detected between a stress condition and the control, with a probability of at least 0.95. The data were deposited into the NCBI Sequence Read Archive under the following accession numbers: control, SRR696127; O_2 + HL, SRR1571498; and HL, SRR1572178.

Results and discussion

Photosynthetic activity under high irradiances
To test the hypothesis that bloom-forming cyanobacteria are better adapted than established model cyanobacteria to environmental stresses such as HL that are characteristic for cells in the surface scum, we compared the photosynthesis at different light intensities (0–1400 μmol photons $m^{-2}s^{-1}$) of *Nodularia* CCY9414 with that of *Synechocystis*. The oxygen evolution rate of *Nodularia* CCY9414 was significantly higher than that of *Synechocystis* from 50 μmol photons $m^{-2}s^{-1}$ upwards at 20 °C and from 100 μmol photons $m^{-2}s^{-1}$ upwards at 30 °C (Supplementary Figure S1a). At both temperatures, *Nodularia* CCY9414 exhibited the greatest difference from *Synechocystis* at the highest measured light intensity. The results of this experiment supported the hypothesis that *Nodularia* CCY9414 has a better capability for using HL intensities for photosynthesis.

To gain insight into the superior light resistance of bloom-forming cyanobacteria, we analyzed *Nodularia* CCY9414 under HL stress, oxidative stress induced by doubling the amount of oxygen partial pressure (+O_2) and under combined light and oxidative stress (HL + O_2) conditions. These stress conditions stimulated photorespiratory activity in *Nodularia* CCY9414 as indicated by the increased glycine/serine ratio (Supplementary Figure S1b), which may be considered as a proxy for increased photorespiration (Allaverdiyeva *et al.*, 2011). In the cells exposed to the +O_2 stress, the highest ratios were detected after 0.5 or 3 h of stress, after which the levels began to decrease. We interpret these findings as an indication of the acclimation of *Nodularia* CCY9414 to the longer-term stress conditions. An increased photorespiratory flux has also been reported for cells of the bloom-forming freshwater cyanobacterium *Microcystis aeruginosa* under HL stress, whereas *Synechocystis* cells do not exhibit such behavior (Meissner *et al.*, 2014).

Stress-related accumulation of selected transcripts
RNA isolated from *Nodularia* CCY9414 cells exposed to a time course of the studied stress conditions was used for an initial qualitative characterization of the stress response by RT-PCR

(Figure 1). Transcript levels of the genes *sod* and *ocp*, which are known to be induced following exposure to HL and $+O_2$ stress in several cyanobacteria (Hihara *et al.*, 2001), increased under all of the selected stress treatments. Under the combined $HL+O_2$ stress, *ocp* showed a higher level of induction compared with *sod*, but the expression of the two genes remained elevated during the entire stress period. Under HL, *ocp* expression was immediately enhanced and then exhibited a declining trend following longer periods of HL exposure, whereas *sod* transcript accumulation peaked at 3 h. The exposure of *Nodularia* to the single $+O_2$ stress condition caused only small changes on *ocp* and *sod* expression (Figure 1a).

Moreover, we analyzed the expression of genes coding for selected enzymes of photorespiratory metabolism, including *pglp*, which codes for the entrance enzyme 2-phosphoglycolate phosphatase, and *glyk*, which codes for the last enzyme in the pathway, glycerate 3-kinase (Eisenhut *et al.*, 2008). In particular, the *glyk* gene showed increased expression under the HL and $HL+O_2$ stresses (Figure 1b), whereas *pglp* induction was less obvious. Finally, we analyzed the expression of *ndaF*, which encodes one subunit of nodularin synthase (Moffitt and Neilan, 2004). Its expression was found to be stimulated after oxidative and HL stresses (Figure 1c), corresponding with the increased amount of toxins that have been reported in cyanobacterial communities under similar conditions (Gehringer and Wannicke, 2014).

Comparative transcriptome analysis

Initial RT-PCR analyses indicated that HL and especially the $HL+O_2$ stress, resulted in the expected cellular response. Therefore, we compared gene expression in non-stressed cells (control) and cells exposed to the studied stress conditions by the transcriptome-wide mapping of TSSs. A total of 38 851 231 sequence reads were obtained for the HL-stressed sample and 39 503 192 reads for the sample exposed to $HL+O_2$ (Supplementary Table S2). These data were compared with a total of 41 519 905 sequence reads from control cells. To exclude very weak or possible false-positive TSSs from this comparison, we chose a more stringent TSS threshold of 620 reads, reducing the number of TSSs from the initial 6519 (Voß *et al.*, 2013) to 3734 for the control cells. However, we also identified 849 and 746 previously unknown additional TSSs that were active after 3 h HL and 0.5 h $HL+O_2$, respectively. Among them, 300 TSSs were stimulated by both stresses, altogether leading to a total of 5029

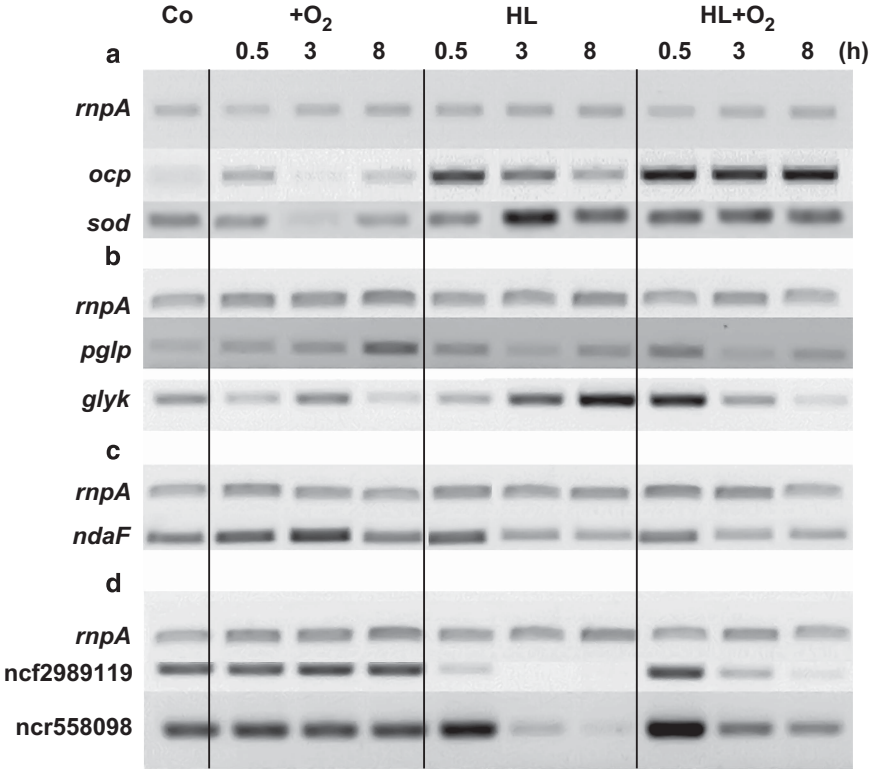

Figure 1 Semi-quantitative analysis of the expression of selected genes in cells of *N. spumigena* CCY9414 by RT-PCR. Shown are RT-PCR results after exposure to an enhanced oxygen concentration ($+O_2$; 40%), HL (1200 μmol photons $m^{-2}s^{-1}$) or both stresses combined ($HL+O_2$) for a period of 0.5, 3 or 8 h. RNase P mRNA (*rnpA)* was amplified for control. Expression of these genes in control cells (Co) is shown in the first lane. (**a**) Transcript accumulation for the orange carotenoid protein (*ocp*) and the superoxide dismutase subunit B (*sodB*) as markers for oxidative stress. (**b**) Transcript accumulation for the phosphoglycolate phosphatase (*glgp*) and glycerate 3-kinase (*glyk*) as markers for photorespiration. (**c**) Transcript accumulation for the nodularin synthase gene F (*ndaF*) as marker for the toxin synthesis. (**d**) Transcript accumulation for selected ncRNAs.

TSSs in this study (Supplementary Table S3). The activation of a high number of additional TSSs under various stress conditions has also been found for *Synechocystis* (Kopf *et al.*, 2014). The highest expression levels in *Nodularia* CCY9414 (measured as absolute read counts) were found for the 16S rRNA operons, several ribosomal protein genes, the stress-induced genes *psbA* and NSP_41850, which codes for a chlorophyll-binding protein (CAB)/ELIP/HL-inducible protein family, as well as the ncRNA ncf4097441 (Figure 2). The TSSs were classified as gTSSs (protein-coding mRNAs), iTSSs (TSSs within protein-coding regions), aTSSs (for antisense RNAs) and nTSSs (for ncRNAs within intergenic regions) (Table 1, Figure 3 and Supplementary Table S2).

Recently, the activities of thousands of TSSs have been studied in the marine filamentous cyanobacterium *Trichodesmium erythraeum*, in which 26.7% of the mapped 6080 TSSs active under standard growth conditions were nTSSs (Pfreundt *et al.*, 2014). However, the 12.4% nTSSs in *Nodularia* CCY9414 observed in this study is similar to what has been previously reported in other cyanobacteria, for example, 12.1% in *Synechocystis* (Kopf *et al.*, 2014) and 10.3% in *Anabaena* PCC7120 (Mitschke *et al.*, 2011b). Thus, the composition of the *Nodularia* CCY9414 primary transcriptome resembles that of other cyanobacteria, whereas that of the *Trichodesmium* transcriptome differs.

The full list of 5029 identified TSSs together with their expression levels are presented in Supplementary Table S3. We have provided a visualization of all mapped reads alongside the genome, including all identified TSSs, ncRNAs and asRNAs, as Supplementary Data 1, which is searchable with *Nodularia* CCY9414 locus tags and gene names.

Our data set allowed for the identification of strongly up- and downregulated TSSs under the HL and combined HL + O_2 stress conditions (Supplementary Tables S4 and S5). Using a 3-fold change in expression as threshold, 30 gTSSs showed increased transcription under both stresses (Table 2). A much higher number of gTSSs (105) responded specifically to the combined application of the HL + O_2 stress (Table 3), whereas only 37 gTSSs are specifically regulated by HL alone (Table 4). These changes were statistically robust as revealed by the empirical Bayes analysis of sequence counts (Wu *et al.*, 2010). More genes were likely undergoing increased transcription, particularly those situated downstream in operons; however, our method only detected the 5′-ends of the primary transcripts. Orthologs for 18 out of the 29 genes listed in Table 2 have also been shown to be HL-induced in the model cyanobacterium *Synechocystis* (comparisons were performed using the CyanoEXpress database: http://193.136.227.181/cgi-bin/gx2?n=environmental; Hernandez-Prieto and Futschik, 2012). These similarities indicate that our stress conditions and time points were carefully selected and allowed for a reliable characterization of the transcriptome associated with stress acclimation in *Nodularia* CCY9414.

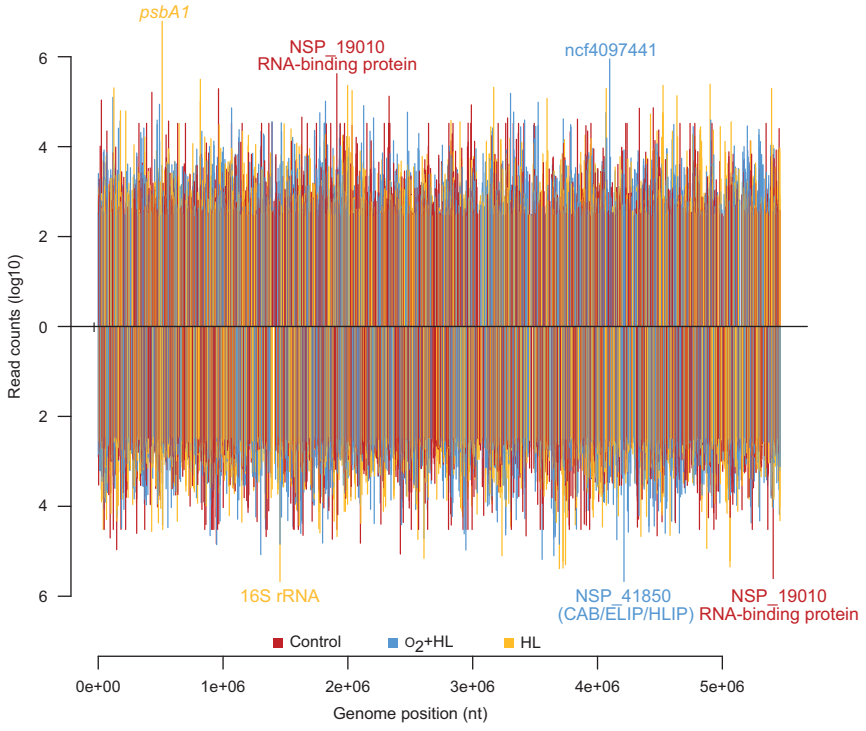

Figure 2 Global overview of all TSS with >620 reads along the chromosome draft sequence (upper part, forward strand; lower part, reverse strand). The TSSs are color-coded according to the respective condition in which they were maximal and selected examples are annotated. For details of all mapped TSSs, see Supplementary Table S3.

Many of the genes listed in Table 2 code for proteins that have important roles in HL and oxidative stress acclimation. Among them, the D1 protein of PS2 encoded by the *psbA* gene is known to be the primary target of these stresses (Mulo *et al.*, 2012). Special D1 protein forms are expressed in model cyanobacteria under stress conditions, such as HL (Garczarek *et al.*, 2008) or anoxia (Summerfield *et al.*, 2008; Sicora *et al.*, 2009). In *Nodularia* CCY9414, the *psbA* gene family consists of four members. All four genes (*psbA1-4*) are transcribed from single TSSs as monocistronic transcripts. One of these genes (*psbA1*, NSP_5370) represented >90% of all reads associated with the four *psbA* genes but was only weakly stimulated by the HL and HL + O_2 stress conditions. Similarly, the *psbA2* gene (NSP_35290) was relatively strongly but constitutively expressed. In contrast, the *psbA3* and *psbA4* genes (NSP_14420 and NSP_33570) were induced by both stress conditions (5- to 14-fold). Interestingly, there are no specialized forms of D1 proteins in *Nodularia* CCY9414 and the proteins encoded by *psbA1-4* have identical amino acid sequences. Moreover, the D1 protein in *Nodularia* CCY9414 exhibits sequence characteristics that set it apart from its orthologs in model cyanobacteria. It's sequence is 10% divergent from the D1 proteins encoded by *psbA2/3* in *Synechocystis*. It is tempting to speculate that the D1 protein encoded by *psbA1-4* share an amino acid sequence optimally adapted to HL conditions. We conclude that *Nodularia* CCY9414 uses a unique strategy to cope with HL-induced damage to PS2 and the D1 protein, because it expresses a presumably HL-adapted D1 protein form from multiple gene copies, some of which are induced under stress conditions serving as backups.

In addition to *psbA*, *sod* and *ocp*, five genes coding for small CABs, one gene coding for the NDH complex and one coding for the chaperone DnaJ were prominently expressed (Table 2). CABs are binding proteins for chlorophyll *a* and carotenoids (Funk and Vermaas, 1999). These proteins are rapidly induced by light stress (also called HL-inducible proteins) and have been suggested to confer protection to the photosynthetic apparatus against oxidative damage (reviewed in Engelken *et al.*, 2012). *Nodularia* CCY9414 possesses nine such genes plus a gene coding for a ferrochelatase–CAB hybrid protein compared with the four CAB genes and one encoding a ferrochelatase–CAB hybrid that have been described in *Synechocystis.* A *Synechocystis* mutant lacking all four of these HL-inducible proteins has been reported, which is sensitive to HL (He *et al.*, 2001; Xu *et al.*, 2004). The presence of twice as many CAB genes in *Nodularia* CCY9414 compared with *Synechocystis* suggests that these proteins may have important roles in conferring greatly increased resilience to HL stress. An increased number of CAB genes have also been reported in HL-adapted compared with low-light-adapted *Prochlorococcus* strains (Scanlan *et al.*, 2009).

Nodularia CCY9414 exhibited the activated expression of many additional genes (for example, coding for adenosine deaminase, which is a peptidoglycan-binding protein) that did not have homologs in the smaller genome of the model cyanobacterium *Synechocystis* or were not previously known to be regulated by HL or HL + O_2 stress (Table 2). The overlap with the already known stress-induced genes became much smaller when those genes were

Table 1 Overview of total numbers of the TSS mapping (relative proportion in brackets in %) via the differential RNAseq approach

	Control	*HL + O_2 stress*	*HL stress*	*Total*
gTSS	1055 (28.25)	1257 (32.79)	1092 (30.06)	1472 (29.27)
aTSS	1104 (29.57)	1014 (26.45)	1022 (28.13)	1460 (29.03)
iTSS	1084 (29.03)	1049 (27.37)	1055 (29.04)	1478 (29.39)
nTSS	491 (13.15)	513 (13.38)	464 (12.77)	619 (12.31)
Sum	3734	3833	3633	5029

Abbreviations: HL, high light; RNAseq, RNA sequencing; TSS, transcription start site.

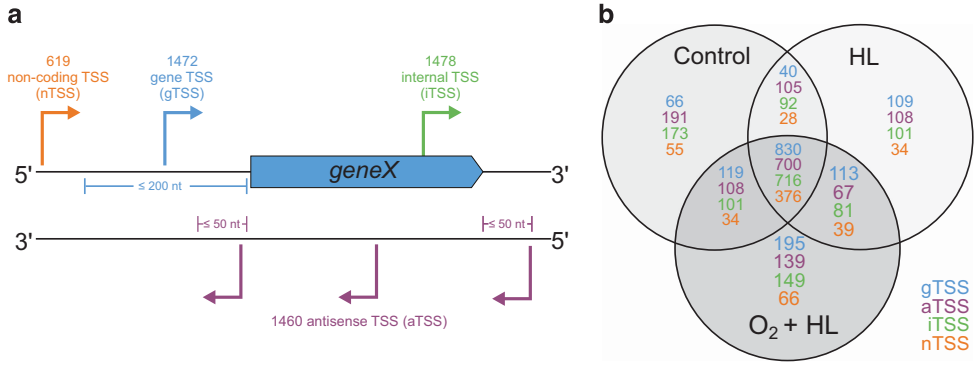

Figure 3 Definition and specificities of the identified TSSs. (**a**) Details of annotation and classification of 5029 TSS into 1472 putative gTSS giving rise to mRNA, 1460 aTSS producing asRNA, 1478 iTSS for internal sense transcripts and 619 nTSS for candidate ncRNAs. aTSS was classified as gTSS when the TSS was located 1–200 nt upstream and in the same orientation as an open reading frame (ORF). TSSs located antisense to an annotated gene or within ≤50 bp 5′ or 3′ to it on the reverse strand were classified as aTSS. TSSs positioned within an annotated gene were classified as iTSS and all remaining TSSs as nTSS from which ncRNAs originate. (**b**) Overlaps and specificities of the different types of TSSs in the three compared conditions.

Table 2 Protein-coding genes whose TSS showed a more than threefold increase in the number of reads

Protein in Nodularia *CCY9414*	*Absolute read counts (control)*	*FC HL + O_2/ control*	*ASC DE probability O_2 + HL/ control*	*FC HL/ control*	*ASC DE probability HL/control*	*Annotation*	*ORF in 6803 (e-value)*
NSP_44260	1	555	1.0	542.5	1.0	Hypothetical protein	Slr0270 (e^{-34})
NSP_9140	47	83.7	1.0	54.5	1.0	Processing peptidase-like protein	Sll0055 (e^{-163})
NSP_27800	293	57.6	1.0	5.2	1.0	CAB/ELIP/HLIP superfamily protein	Ssr2595^{HL} (e^{-29})
NSP_44180	725	38	1.0	19.3	1.0	NADH dehydrogenase I subunit 4. Involved in cyclic electron flow	Slr1291^{HL} (0.0)
NSP_4910	1175	26.3	1.0	10.9	1.0	Ubiquinone biosynthesis monooxygenase UbiB, or ABC1-domain containing ABC transporter	Sll0005^{HL} (0.0)
NSP_48910	988	4.1	1.0	23.8	1.0	CAB/ELIP/HLIP superfamily protein	Ssl1633^{HL} (e^{-14})
NSP_32430	7791	19.6	1.0	9.2	1.0	Orange carotenoid protein	Slr1963^{HL} (e^{-130})
NSP_46960	189	14.9	1.0	19.3	1.0	Zn-dependent proteases	Sll0528^{HL} (e^{-137})
NSP_9460	409	14.2	1.0	8	1.0	Phycoerythrin linker protein CpeS, or, chromophore lyase CpcS	Slr2049 (e^{-10})
NSP_14420	2282	7.6	1.0	14.2	1.0	Photosystem II protein D1 (*psbA3* gene)	Slr1311 (0.0) Sll1867^{HL} (0.0)
NSP_5400	2170	12	1.0	5.8	1.0	Recombination protein RecR	None
NSP_39950	396	11.8	1.0	6.1	1.0	Solanesyl diphosphate synthase	Slr0611^{HL} (e^{-125})
NSP_51570	135	10.2	1.0	9	1.0	2-Octaprenyl-6-methoxyphenol hydroxylase	Slr1300 (e^{-146})
NSP_44510	557	7.5	1.0	9.8	1.0	Adenosine deaminase	None
NSP_3210	249	4.6	1.0	9	1.0	Hypothetical protein	Slr0217 (e^{-42})
NSP_41850	54170	8.7	1.0	5.8	1.0	CAB/ELIP/HLIP superfamily protein	Ssr2595^{HL} (e^{-25})
NSP_42110	4661	8.1	1.0	6.8	1.0	Beta-carotene ketolase/hydroxylase, or, fatty acid desaturase	Sll1468 (e^{-05})
NSP_33570	2709	7	1.0	5.5	1.0	Photosystem II protein D1 (*psbA4* gene)	Slr1311 (0.0) Sll1867^{HL} (0.0)
NSP_9820	696	6.4	1.0	3.5	1.0	DNA-binding, ferritin-like protein Dps (oxidative damage)	Slr1894 (e^{-09})
NSP_17520	6085	3.1	1.0	6.4	1.0	CAB/ELIP/HLIP superfamily protein	Ssl1633^{HL} (e^{-16})
NSP_46010	22114	5.4	1.0	6.2	1.0	CAB/ELIP/HLIP superfamily protein	Ssl1633^{HL} (e^{-15})
NSP_32830	789	3.5	1.0	5.4	1.0	GTP cyclohydrolase I	Slr0426^{HL} (e^{-100})
NSP_9990	499	4.8	1.0	5.3	1.0	Peptidoglucan-binding protein	None
NSP_48320	696	3.3	1.0	5.3	1.0	CopG family transcriptional regulator	Ssr5117 (e^{-26})
NSP_7660	347	5.2	1.0	4.8	1.0	Chaperone protein DnaJ	Sll0897^{HL} (e^{-177})
NSP_29690	677	4.5	1.0	4.5	1.0	Hypothetical protein; possible iron–sulfur cluster-binding protein	Sll1697^{HL} (e^{-166})
NSP_31650	442	3.5	1.0	4.3	1.0	Superoxide dismutase [Fe]	Slr1516^{HL} (e^{-88})
NSP_8400	427	4.1	1.0	3.4	1.0	Hypothetical protein	None
NSP_1700	607	3.2	1.0	4.1	1.0	Beta-carotene hydroxylase	Sll1468^{HL} (e^{-148})
NSP_46010	445	3.4	1.0	3.3	1.0	CAB/ELIP/HLIP superfamily protein	Ssl1633^{HL} (e^{-15})

Abbreviations: ASC, analysis of sequence counts; DE, differentially expressed; ELIP, early light induced protein; FC, fold change; HL, high light; HLIP, HL-inducible protein; ORF, open reading frame; TSS, transcription start site.
Protein-coding genes whose TSS showed a more than threefold increase in the number of reads under HL stress for 3 h as well as under combined oxidative and HL ($HL + O_2$) stress for 0.5 h (minimum number of 620 reads at both conditions).
For comparison, the orthologs in *Synechocystis* are given and indicated by the suffix HL when these genes were HL-induced in *Synechocystis* microarray data sets (CyanoEXpress 1.2 database; Hernandez-Prieto and Futschik, 2012). For the complete list of TSSs see Supplementary Table S3.

considered, which were particularly induced either by the HL or the $HL + O_2$ stress (orthologs for only 20% and 8.6% of the genes listed in Tables 3 and 4, respectively, are also HL-induced in *Synechocystis*). Among these genes, many code for hypothetical proteins, that is, their functions have not yet been described in model organisms. It is not unlikely that some of these proteins are involved in stress acclimation, contributing to the bloom-forming capability of *Nodularia* CCY9414 in a yet unknown manner. Another group of genes particularly induced following exposure to the combined $HL + O_2$ stress included those coding for proteins that function in DNA structure maintenance or modification, such as uracil–DNA glycosylase, DNA methylase and nuclease. Interestingly, genes coding for two phage integrases also showed higher transcript levels in the stressed *Nodularia* CCY9414 cells. Cyanophages have been reported to be crucial factors that determine the fates of toxic cyanobacterial blooms (Yoshida-Takashima *et al.*, 2012). Finally, the TSS of the *ndaA* gene, which is the first gene in the operon coding for the huge nodularin synthetase complex (Moffitt and Neilan, 2004), showed threefold higher expression (corresponding to higher amounts of *ndaF* in our RT-PCR experiments, see Figure 1c), indicating an increase in nodularin synthesis under bloom-forming conditions. The crucial role of toxins in the

Table 3 Protein coding genes whose TSS showed a more than threefold increase in the number of reads

Protein in Nodularia CCY9414	*Absolute read counts (control)*	*FC HL+ O_2/ control*	*ASC DE probability O_2+HL/ control*	*FC HL/ control*	*ASC DE probability HL/control*	*Annotation*	*ORF in 6803 (e-value)*
NSP_50790	1	1334	1.0	1	0.0	Glycosyl transferase, group 1	Sll0045 (e^{-30})
NSP_43710	20	50.3	1.0	0.1	0.0	LSU ribosomal protein L5p (L11e)	Sll1808 (e^{-108})
NSP_41430	96	18.9	1.0	0.9	0.0	4Fe–4S ferredoxin, nitrogenase-associated	Sll0741 ($2e^{-08}$)
NSP_16900	109	13.3	1.0	0.9	0.0	Hypothetical protein	None
NSP_24490	89	13.1	1.0	1.1	0.0	Phytoene synthase	Slr1255 ($2e^{-135}$)
NSP_14160	338	12.7	1.0	0.6	0.0	Cytochrome b559 α-Chain (PsbE)	Ssr3451 ($2e^{-45}$)
NSP_3790	142	10.2	1.0	2	0.61	Photosystem I subunit IX (PsaJ)	Sml0008 ($2e^{-04}$)
NSP_6400	149	9.8	1.0	2.9	1.0	NifU-like protein	Ssl2667 (e^{-43})
NSP_18580	409	9.3	1.0	0.5	0.0	General secretion pathway protein H, Type IV pilin PilA	Sll1694^{HL} (e^{-32})
NSP_2690	384	8.8	1.0	0.2	0.0	Hypothetical protein	Slr1900 (e^{-49})
NSP_22750	299	7.9	1.0	0	0.0	WD repeat-containing protein	Slr8038 ($3e^{-39}$)
NSP_47150	203	7.4	1.0	1	0.0	Hypothetical protein	None
NSP_6930	206	7.3	1.0	1.2	0.0	Hypothetical protein	None
NSP_9450	1264	6.9	1.0	2.9	1.0	RND efflux membrane fusion protein	Sll0141 (e^{-83})
NSP_45100	200	6.8	1.0	1.3	0.0	Phycoerythrin linker protein CpeS homolog	Slr2049 (e^{-59})
NSP_38040	217	6.6	1.0	2.4	1.0	Hypothetical protein	None
NSP_48690	450	6.3	1.0	1.5	0.0	Protein CP12, regulation of Calvin cycle	Ssl3364 ($2e^{-21}$)
NSP_49270	178	6.1	1.0	2.6	1.0	WD40 repeat	Sll0877 ($2e^{-77}$)
NSP_19890	226	5.9	1.0	1.1	0.0	Ferric uptake regulation protein	Sll1937 ($2e^{-06}$)
NSP_33730	341	5.6	1.0	2.1	0.94	Dihydroxy-acid dehydratase	Slr0452 (0.0)
NSP_14650	306	5.5	1.0	0.1	0.0	Major facilitator family transporter	Sll1154 (e^{-112})
NSP_10860	578	5.4	1.0	0.7	0.0	Carbohydrate-selective porin. OprB family	Sll0772 (e^{-98})
NSP_36640	195	5.4	1.0	0.4	0.0	Hypothetical protein	None
NSP_31680	704	5.4	1.0	2.5	1.0	PHP family metal-dependent phosphoesterase	Sll0549 (e^{-73})
NSP_34350	677	5.3	1.0	1.1	0.0	Hypothetical protein	Slr2073 ($3e^{-49}$)
NSP_19030	308	5.3	1.0	2.5	1.0	Hypothetical protein	Slr1391 (e^{-16})
NSP_15460	1702	5.3	1.0	0.6	0.0	ATPase involved in DNA repair	None
NSP_700	368	5.1	1.0	0.7	0.0	Uracil–DNA glycosylase, family 4	None
NSP_42260	614	5	1.0	1.6	0.0	Chorismate synthase	Sll1747 (0.0)
NSP_48530	992	4.9	1.0	1.1	0.0	Cell division trigger factor (EC 5.2.1.8)	Sll0533^{HL} (e^{-125})
NSP_52140	387	4.8	1.0	0.5	0.0	Sigma54 homolog	Ssr0657 ($3e^{-32}$)
NSP_33420	320	4.8	1.0	0.9	0.0	Hypothetical protein	Slr0975 ($6e^{-117}$)
NSP_24390	434	4.7	1.0	1.1	0.0	NADH dehydrogenase I subunit 4, PS1 cyclic electron flow	Slr1291^{HL} (0.0)
NSP_50790	1	4.7	1.0	2.4	NA	Glycosyl transferase, group 1	Sll0045 ($2e^{-30}$)
NSP_40430	248	4.6	1.0	0.7	0.0	Protein of unknown function DUF820	Slr1613 ($3e^{-44}$)
NSP_42360	322	4.6	1.0	0.6	0.0	Nucleoside triphosphate pyrophosphohydrolase MazG	Sll1005^{HL} (e^{-121})
NSP_15410	281	4.5	1.0	0.7	0.0	ATPase associated with various activities or gas vesicle protein GvpN	Slr1416 (e^{-05})
NSP_35650	417	4.5	1.0	0.9	0.0	Hypothetical protein	None
NSP_14220	4891	4.4	1.0	1.1	0.0	Transposase. IS605 OrfB	None
NSP_25450	638	4.4	1.0	1	0.0	Hypothetical protein	None
NSP_48520	453	4.3	1.0	1.2	0.0	ATP-dependent Clp protease proteolytic subunit (EC 3.4.21.92)	Sll0534 (e^{-125})
NSP_1470	356	4.3	1.0	2.2	0.99	Hypothetical protein	None
NSP_27850	1945	4.2	1.0	0.3	0.0	TldD protein, part of proposed TldE/TldD proteolytic complex	Slr1322 (0.0)
NSP_35830	777	4.2	1.0	1.5	0.0	Hemolysin-like	Slr0483 (e^{-38})
NSP_42990	333	4.2	1.0	2.6	1.0	Nuclease subunit of the excinuclease complex	Slr1035 (e^{-12})
NSP_10200	1257	4.1	1.0	1.1	0.0	Hypothetical protein	Slr0575 (e^{-78})
NSP_47200	6886	4.1	1.0	0.5	0.0	Hypothetical protein	Sll0749 (e^{-38})
NSP_39370	265	4	1.0	1.2	0.0	Dihydrolipoamide dehydrogenase	Slr1096 (0.0)
NSP_10630	444	4	1.0	2.2	1.0	ATP-dependent peptidase S16	Sll0195 (e^{-117})
NSP_17370	303	4	1.0	2	0.92	ATP-dependent Clp protease proteolytic subunit (EC 3.4.21.92)	Slr0164 (e^{-99})
NSP_15490	549	3.9	1.0	1	0.0	Cell division control protein FtsH	Slr0228^{HL} (e^{-58})
NSP_17490	2512	3.9	1.0	2.1	1.0	Hypothetical protein	Sll1483^{HL} (e^{-43})
NSP_48980	1335	3.9	1.0	0.8	0.0	Hypothetical protein	None
NSP_46280	1582	3.9	1.0	1.2	0.0	3-oxoacyl-[acyl-carrier protein] reductase (EC 1.1.1.100)	Sll0330 (e^{-17})
NSP_16440	414	3.9	1.0	1.8	0.13	Hypothetical protein	None
NSP_33860	721	3.9	1.0	1.1	0.0	Putative protein	Slr1378 (e^{-75})
NSP_830	283	3.8	1.0	0.9	0.0	Octaprenyl-diphosphate synthase (EC 2.5.1.-)/ Geranylgeranyl pyrophosphate synthetase	Slr0739 (e^{-156})
NSP_51180	279	3.8	1.0	0.7	0.0	Hypothetical protein	None
NSP_4850	268	3.8	1.0	0.2	0.0	EsV-1-176	Slr0645 ($2e^{-94}$)
NSP_53130	640	3.7	1.0	0.5	0.0	Translation IF3	Slr0974 (e^{-26})
NSP_50960	510	3.7	1.0	1.4	0.0	Hypothetical protein	None
NSP_1350	1083	3.7	1.0	0.7	0.0	Hypothetical Protein	Slr0476^{HL} ($9e^{-15}$)

Table 3 (Continued)

Protein in Nodularia CCY9414	*Absolute read counts (control)*	*FC HL+ O_2/ control*	*ASC DE probability O_2+HL/ control*	*FC HL/ control*	*ASC DE probability HL/control*	*Annotation*	*ORF in 6803 (e-value)*
NSP_38540	1663	3.7	1.0	0.4	0.0	Photosystem II protein PsbK	Sml0005 (e^{-13})
NSP_3140	1342	3.7	1.0	0.5	0.0	Hypothetical protein	None
NSP_50680	446	3.6	1.0	1.5	0.0	Glycogen phosphorylase (EC 2.4.1.1)	Slr1367 (e^{-18})
NSP_25450	638	3.6	1.0	2.2	0.0	Hypothetical protein	None
NSP_51790	945	3.6	1.0	1.4	0.0	Cytochrome b6-f complex iron-sulfur subunit PetC1 (Rieske)	Sll1316 (e^{-98})
NSP_36900	814	3.6	1.0	1	0.0	Peptidoglycan-binding domain 1	None
NSP_30660	517	3.6	1.0	1.9	0.59	Hypothetical protein	None
NSP_51310	1074	3.6	1.0	1.4	0.0	Ton-B like periplasmic protein	None
NSP_19230	4411	3.5	1.0	1.1	0.0	Hypothetical protein	Slr2070 (e^{-61})
NSP_51330	368	3.5	1.0	0.2	0.0	Phage shock protein A	Sll0617 (e^{-85})
NSP_46110	555	3.5	1.0	1.2	0.0	NADH dehydrogenase (EC 1.6.99.3), NdhD	Slr1743 (e^{-170})
NSP_52960	1906	3.5	1.0	0.9	0.0	Shikimate kinase I (EC 2.7.1.71)	Sll1660 (e^{-70})
NSP_30840	381	3.5	1.0	1.5	0.0	NAD (P) transhydrogenase alpha subunit (EC 1.6.1.2)	Slr1239 (e^{-107})
NSP_52090	313	3.5	1.0	0.9	0.0	Two-component response regulator	Slr1909 (e^{-109})
NSP_25460	964	3.5	1.0	1.7	0.0	Oxidoreductase, Gfo/Idh/MocA family	Slr0338 (0.0)
NSP_15680	3773	3.4	1.0	1.1	0.0	Hypothetical protein	Slr2025 (e^{-37})
NSP_51030	335	3.4	1.0	2	0.71	Hypothetical protein	None
NSP_43620	299	3.4	1.0	0.5	0.0	Large SU ribosomal protein L36p	Sml0006 (e^{-17})
NSP_41520	335	3.3	1.0	2.1	0.96	Photosystem I P700 chlorophyll a apoprotein subunit Ia (PsaA)	Slr1834^{HL} (0.0)
NSP_16880	962	3.3	1.0	1.8	0.11	Sorbitol dehydrogenase (EC 1.1.1.14)	Sll0990 (e^{-13})
NSP_40730	1758	3.3	1.0	1.7	0.0	DNA methylase N-4/N-6	None
NSP_26680	734	3.3	1.0	2.2	1.0	Phage integrase	None
NSP_33380	1633	3.3	1.0	1.7	0.0	Chaperone protein DnaK	Sll1932 (0.0)
NSP_7750	464	3.3	1.0	0.3	0.0	Iron (III)-traNSP_ort ATP-binding protein SfuC	Slr0354 (e^{-101})
NSP_9910	2965	3.3	1.0	1.3	0.0	Hypothetical protein	None
NSP_38190	375	3.3	1.0	2	0.88	Similar to Ymc	None
NSP_19230	4411	3.2	1.0	1	0.0	Hypothetical protein	Slr2070 ($2e^{-67}$)
NSP_22130	7582	3.2	1.0	1.1	0.0	Hypothetical protein	None
NSP_300	403	3.2	1.0	2.1	0.98	3-Polyprenyl-4-hydroxybenzoate carboxy-lyase	Sll0936 (0.0)
NSP_19990	736	3.2	1.0	1.6	0.0	ADP-heptose–lipooligosaccharide heptosyl-transferase II (EC 2.4.1.-)	Slr0606 (e^{-101})
NSP_24440	328	3.2	1.0	2.3	1.0	Hypothetical protein	None
NSP_37380	514	3.1	1.0	0.1	0.0	ATP synthase β-chain (EC 3.6.3.14)	Slr1329^{HL} (0.0)
NSP_45180	2481	3.1	1.0	2.7	1.0	Carboxyl-terminal processing protease	Slr0008 (e^{-171})
NSP_1410	1125	3.1	1.0	1.2	0.93	Ribulose-phosphate 3-epimerase (EC 5.1.3.1)	Sll0807 (e^{-144})
NSP_12600	483	3.1	1.0	0.6	0.0	Hypothetical protein	Sll1381 ($3e^{-53}$)
NSP_50770	1649	3.1	1.0	0.8	0.0	RNA-binding protein	Slr0193 (e^{-48})
NSP_890	591	3.1	1.0	1.5	0.0	Flavodoxin reductases (ferredoxin–NADPH reductases) family 1	Sll0765 (e^{-110})
NSP_50880	1046	3	1.0	0.6	0.0	Phage integrase	None
NSP_42140	351	3	1.0	0.3	0.0	Amino acid adenylation protein NdaA involved in nodularin synthesis	None
NSP_6650	927	3	1.0	0.9	0.0	Serine/threonine kinase	Sll1380 (e^{-23})
NSP_29410	734	3	1.0	0.7	0.0	Hypothetical protein	Sll1142 (e^{-82})
NSP_1450	1317	3	1.0	0.3	0.0	Acetolactate synthase large subunit (EC 2.2.1.6)	Slr2088 (0.0)
NSP_2440	424	3	1.0	0.8	0.0	Hypothetical protein	Sll1022 (e^{-82})

Abbreviations: ASC, analysis of sequence counts; DE, differentially expressed; ELIP, early light induced protein; FC, fold change; HL, high light; IF3, initiation factor 3; LSU, large subunit; ORF, open reading frame; RND, resistance-nodulation-cell division; WD, Trp-Asp.
Protein coding genes whose TSS showed a more than threefold increase in the number of reads specifically under combined HL and oxygen ($HL+O_2$) stress (minimum number of 620 reads at combined $HL+O_2$ stress).
For comparison, the expression levels after HL stress in *Nodularia* CCY9414 as well as the orthologs in *Synechocystis* are given. Genes were indicated by the suffix HL, when they were HL-induced in *Synechocystis* according to microarray data sets (CyanoEXpress 1.2 database; Hernandez-Prieto and Futschik, 2012). For the complete list of TSSs see Supplementary Table S3.

HL resistance of bloom-forming cyanobacteria has been shown for the freshwater cyanobacterium *M. aeruginosa* that accumulates the hepatotoxin microcystin, which is similar to nodularin. Microcystin seems to have an important role in HL resistance due to its binding to the main carboxylating enzyme Rubisco (Zilliges *et al.*, 2011). In addition, the increased expression of genes coding for a number of proteins that are involved in enzymatic reactions as well as transport processes (for example, iron (*tonB*-like) and manganese transporters) was also observed. These changes indicate that stress situations resembling bloom-forming conditions induce complex metabolic reorganization.

In anaerobic phototrophic bacteria, ncRNAs have been characterized as important regulators of the

Table 4 Protein coding genes whose TSS showed a more than threefold increase in the number of reads specifically under high light (HL) stress (minimum number of 1000 reads at HL stress)

Protein in Nodularia CCY9414	*Absolute read counts (Control)*	*FC HL+ O_2/ control*	*ASC DE probability O_2+HL/ control*	*FC HL/ control*	*ASC DE probability HL/control*	*Annotation*	*ORF in 6803 (e-value)*
NSP_3660	1	0.5	0.0	502.5	1.0	ATP-dependent DNA helicase RecQ	Slr1536 ($4e^{-69}$)
NSP_44910	22592	2.1	1.0	10.2	1.0	Phycobilisome degradation protein NblA	Ssl0453 (e^{-04})
NSP_16590	901	0.3	0.0	10.0	1.0	(Manganese) ABC transporter. ATP-binding protein	Sll0489 (e^{-09})
NSP_31420	533	2.4	1.0	6.2	1.0	Ribose-phosphate pyrophosphokinase	Sll0469 (0.0)
NSP_45620	202	2.05	0.65	5.72	1.0	NADH dehydrogenase subunit 2	Sll0223^{HL} (0.0)
NSP_10590	1417	2.8	1.0	5.7	1.0	Translation elongation factor G	Sll1098 (0.0)
NSP_31650	2630	2.77	1.0	5.45	1.0	Superoxide dismutase [Fe] (EC 1.15.1.1)	Slr1516 ($5e^{-87}$)
NSP_36400	213	1.39	0.0	4.92	1.0	COG2931: RTX toxins and related Ca^{2+}-binding proteins	None
NSP_26350	409	2.3	1.0	4.8	1.0	Ribosomal protein L11 methyltransferase	Sll1909 (e^{-135})
NSP_46680	220	0.38	0.0	4.62	1.0	Hypothetical protein	Slr5058 ($9e^{-79}$)
NSP_450	7516	1.2	0.0	4.4	1.0	Alkyl hydroperoxide reductase subunit Cell wall binding protein	None
NSP_600	311	0.3	0.0	4.3	1.0	Probable iron binding protein, HesB_IscA_SufA family	Slr1417 ($1e^{-61}$)
NSP_4830	384	1.7	0.0	4.2	1.0	Hypothetical protein	None
NSP_3830	284	2.4	1.0	4.2	1.0	Enolase (EC 4.2.1.11)	Slr0752 (0.0)
NSP_53110	2651	2.8	1.0	4.0	1.0	Hypothetical protein	None
NSP_36850	51014	2.2	1.0	3.9	1.0	Hypothetical protein	Slr1676^{HL} (e^{-59})
NSP_16910	382	1.4	0.0	3.9	1.0	Serine/threonine kinase	Slr0599 (e^{-67})
NSP_39220	494	0.8	0.0	3.7	1.0	Putative anti-sigma factor antagonist	Ssr1600 (e^{-50})
NSP_11290	6147	2.2	1.0	3.7	1.0	Photosystem II protein D2 (PsbD)	Slr0927 (0.0)
NSP_4280	797	1.3	0.0	3.5	1.0	Two-component system, regulatory protein	Slr1042 ($5e^{-67}$)
NSP_3570	548	2.5	1.0	3.4	1.0	Sulfur acceptor protein SufE iron-sulfur cluster assembly	Sll1151 (e^{-173})
NSP_6070	775	1.6	0.0	3.3	1.0	Hypothetical protein	Sll2002 (e^{-115})
NSP_9380	1437	2.7	1.0	3.3	1.0	LSU ribosomal protein L11p (L12e)	Sll1743^{HL} ($5e^{-84}$)
NSP_44900	17518	1.44	0.0	3.29	1.0	Hypothetical protein	None
NSP_39280	379	1.9	0.27	3.3	1.0	tRNA:m (5)U-54 MTase gid	Sll0204 (0.0)
NSP_44740	351	1.6	0.0	3.3	1.0	Omega-3 fatty acid desaturase	Sll1441^{HL} (e^{-178})
NSP_640	937	1.4	0.0	3.3	1.0	Cell division inhibitor	Slr1223 (e^{-130})
NSP_15880	437	2.1	0.93	3.2	1.0	Acetyltransferase (EC 2.3.1.-)	None
NSP_21560	811	0.4	0.0	3.2	1.0	Putative multicomponent Na+/H+ antiporter subunit C	Slr2006^{HL} (e^{-49})
NSP_19170	786	1.3	0.0	3.2	1.0	Hypothetical protein	Slr0806 (e^{-138})
NSP_7020	1081	2.0	0.75	3.1	1.0	Hypothetical protein	None
NSP_32830	344	2.9	1.0	3.1	1.0	GTP cyclohydrolase I (EC 3.5.4.16)	Slr0426^{HL} ($1e^{-98}$)
NSP_7400	814	2.6	1.0	3.1	1.0	SAM-dependent methyltransferase	None
NSP_1020	472	1.0	0.0	3.1	1.0	Kynurenine 3-monooxygenase (EC 1.14.13.9)	None
NSP_15330	728	2.4	1.0	3.0	1.0	NADP-dependent malic enzyme (EC 1.1.1.40)	Slr0721 (0.0)
NSP_42850	570	0.9	0.0	3.0	1.0	Phenylalanyl-tRNA synthetase α-chain (EC 6.1.1.20)	Sll0454 (0.0)

Abbreviations: ASC, analysis of sequence counts; DE, differentially expressed; FC, fold change; HL, high light; LSU, large subunit; RTX, repeats in toxin; SAM, S-adenosylmethionine.
For comparison, the expression levels after combined HL + O_2 in *Nodularia* CCY9414 as well as the orthologs in *Synechocystis* (indicated, if present, as in Table 2) are given. For the complete list of TSSs see Supplementary Table S3.

response to singlet oxygen (Berghoff *et al.*, 2009). In cyanobacteria, transcriptomic changes under elevated oxygen concentrations have not been addressed to date. Therefore, we focused on the 68 aTSSs and 42 nTSSs that were induced under HL and, in particular, under HL + O_2 conditions (Supplementary Table S6). For example, one aTSS that was induced by 2.5- and 5.4-fold under the HL + O_2 and HL stresses, respectively, was located antisense to the *cpcC* gene coding for the

phycocyanin-associated phycobilisome rod linker polypeptide (Figure 4). Interestingly, the gTSS-driving expression of the *cpcBAC* mRNA was partially inversely regulated and its read count dropped to 0.2 under HL compared with that of the control. We conclude that the asRNA to *cpcC* is likely functionally relevant and may contribute to the repression of *cpcBAC* mRNA specifically under HL. It is known from model strains that HL decreases the phycobilisome antennae size to avoid the over-reduction of PS2 (Kirilovski and Kerfeld, 2012). Interestingly, an ortholog of this asRNA also exists in *Anabaena* PCC7120, in which it seems to decrease *cpcBAC* expression under nitrogen-limiting conditions (Mitschke *et al.*, 2011b). Thus, the functional relationship between the *cpcBAC* gTSS and the *cpcC* aTSS may not be limited to the HL response.

The ncRNA PsrR1 has been characterized in *Synechocystis* as a central regulator for the adaptation of the photosynthetic apparatus to HL (Georg *et al.*, 2014). PsrR1 has been speculated to have similar roles in other cyanobacteria. Indeed, with the ncRNA ncr3914006, *Nodularia* CCY9414 possesses a likely candidate with the typical secondary structure and conserved central sequence element of PsrR1 (Figure 5). This ncRNA was induced 408- and 57-fold under the HL + O_2 and HL stresses (Supplementary Table S3). The much higher induction of PsrR1 expression under HL + O_2 compared with that under HL stress alone may represent an important insight, because the effect of elevated oxygen concentrations has not been analyzed to date. Our data suggest that PsrR1 may possess an even more important function than previously considered, following exposure to combined stresses. In *Synechocystis*, the *psaL* mRNA, which is one of the PsrR1 key targets, is subjected to endonucleoytic cleavage by RNase E at a specific cleavage site located 7 nt downstream of the PsrR1:psaL interaction site (Georg *et al.*, 2014). A comparable mechanism possibly occurs in *Nodularia* CCY9414. The RNA sequencing analysis showed a sharp drop in transcriptome coverage at 7 nt downstream of one of three possible interaction sites (Figure 5c). However, in contrast with what has been reported in *Synechocystis*, this sharp drop in coverage was also observed in the control. Interestingly, two different TSSs drive the transcription of *psaL* in *Nodularia* CCY9414 compared with a single TSS in *Synechocystis.* As both TSSs are repressed by HL, we conclude that the light-dependent repression of *psaL* in *Nodularia* CCY9414 via PsrR1 and transcriptional repression is more pronounced than in *Synechocystis.*

Several of the other ncRNAs likely have important roles as well. For example, the ncRNA that is transcribed from the nTSS at position 3867196r located 199 nt downstream of NSP_38130 is the template repeat RNA of diversity generating retroelement 1 (Voß *et al.*, 2013). In contrast to other

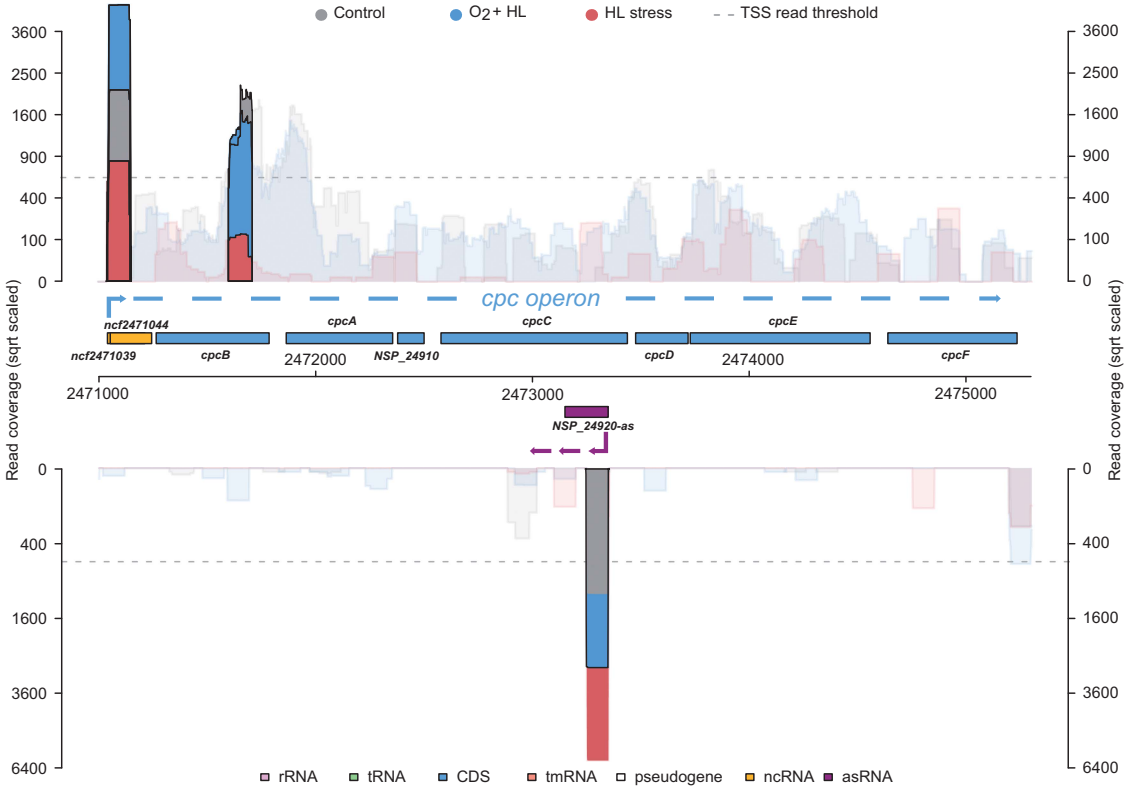

Figure 4 The posttranscriptional silencing of *cpcBAC* mRNA accumulation may involve an asRNA induced under HL. The genes *NSP_24890-NSP_24950* encompassing the genes *cpcBACDEF* and one very short unknown gene are shown. The read accumulation for the two TSS in this region, the gTSS in front of *cpcB* and for the aTSS in *cpcC* are given according to the three investigated conditions.

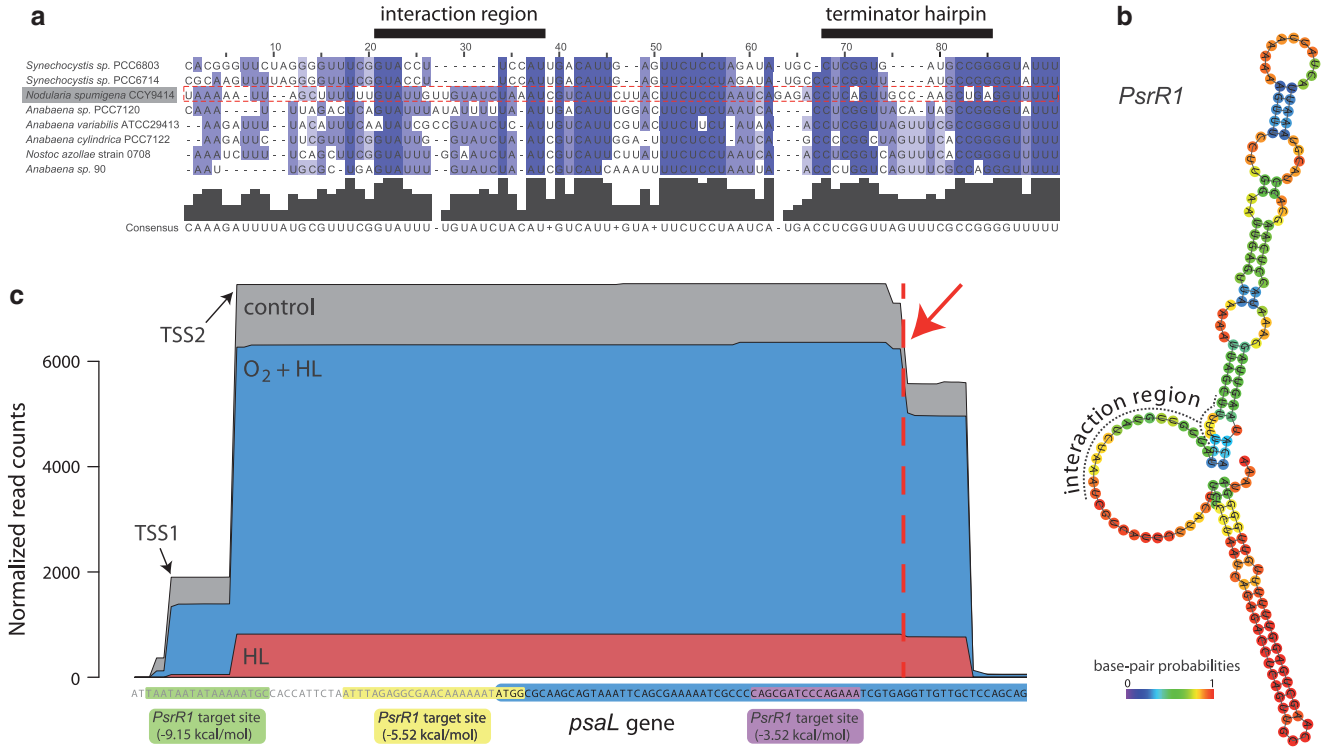

Figure 5 The ncRNA PsrR1 in *N. spumigena* CCY9414 and its major target, the *psaL* gene, encoding subunit XI of PSI. (**a**) Sequence comparison of PsrR1 with its homologs from two strains of *Synechocystis* and five other filamentous cyanobacteria. The regions involved in target interaction and forming a Rho-independent terminator are annotated according to Georg *et al.* (2014). (**b**) Secondary structural model for the *Nodularia* CCY9414 PsrR1. (**c**) Transcript accumulation for the *psaL* mRNA in control and two stress conditions. There are two closely spaced TSSs, at position 4046958 (TSS2) and 4046949 (TSS1) of the reverse strand, indicated by the black arrows. The *psaL* gene is highlighted by a blue box. Three possible sites for the interaction with PsrR1 are given. Sequence coverage shows a sharp drop (marked by a red arrow and vertical line), which indicates a possible processing site due to interaction with PsrR1 (Georg *et al.*, 2014).

bacteria, in which such ncRNAs serve as templates for cDNA synthesis with subsequent recombination into protein-coding regions (Arambula *et al.*, 2013; Pfreundt *et al.*, 2014), this system reported here must target mainly non-coding regions, indicated by 70 nearly identical copies of diversity generating retroelement 1 (Voß *et al.*, 2013). The ncRNA ncf2989119, which showed the sixth to seventh highest levels of expression at the nTSS, is an ortholog of ncRNA T1 in *Anabaena* PCC7120 (Mitschke *et al.*, 2011b), where it is controlled by HetR, the regulator of heterocyst development. Interestingly, the expression of ncf2989119 dropped dramatically under HL, which was also confirmed independently in a time-course experiment (Figure 1d).

Conclusion

Bloom-forming cyanobacteria such as *Nodularia* are expected to be well adapted to stressors, including HL and/or oxidative stress, because these conditions often occur concurrent with the formation of dense scums at the water surface. Our physiological experiments supported this assumption, because the photosynthetic activity remained high even at the highest light intensities. In addition, *Nodularia* CCY9414 showed signs of an increase in photorespiratory flux as have been demonstrated for *M. aeruginosa*, another bloom-forming cyanobacterium (Meissner *et al.*, 2014). Photorespiration cooperates with Mehler-like reactions catalyzed by flavodiiron proteins to dissipate excess absorbed energy in cyanobacteria (Hackenberg *et al.*, 2009; Allahverdiyeva *et al.*, 2011). Activation of this physiological reaction is consistent with our observation of many upregulated genes coding for photorespiratory enzymes and flavodiiron proteins. In addition, genes for toxin synthesis enzymes were also upregulated, implying that these compounds may specifically have an important role in the cellular acclimation to conditions of bloom formation, consistent with previous observations for *Microcystis* (Zilliges *et al.*, 2011).

Our transcriptomics results suggested many additional changes in mRNA levels and also in ncRNA abundance. All mentioned changes are highly supported by statistics and key genes assessed by RT-PCR showed similar trends, validating these results. Accordingly, the RNA sequencing approach allowed the identification of many differentially expressed genes for proteins that might ensure the acclimation of *Nodularia* and related cyanobacteria to the harsh conditions in the surface scum. They are likely important for stress acclimation, because, by analogy, many of the annotated genes code for proteins with known functions in HL and oxidative

stress acclimation in model cyanobacteria such as *Synechocystis*. However, we found many new stress-regulated genes that code for proteins involved in metabolism, transport, DNA stability and structure, and other still-unknown functions. These proteins are likely particularly important for successful bloom formation in *Nodularia* and related cyanobacteria, because they were found specifically induced under conditions characteristic for this ecological situation in *Nodularia* CCY9414 and not before in planktonic, non-blooming cyanobacteria. Our screen for stress-induced ncRNAs revealed several that are important to stress acclimation, including the asRNA associated with the *cpc* operon and PsrR1 associated with photosynthetic genes. Collectively, our physiological and transcriptomic data provide many insights into the complex adaptation of the toxic diazotrophic cyanobacterium *Nodularia* CCY9414 to conditions prevailing under bloom conditions in its natural habitat, the Baltic Sea.

Conflict of Interest

The authors declare no conflicts of interests.

Acknowledgements

We thank Kathrin Jahnke for technical assistance. FM was supported by a scholarship from the INF (Interdisziplinäre Fakultät, Maritime Systeme) of the University Rostock. This work was supported by the EU project MaCuMBA (Marine Microorganisms: Cultivation Methods for Improving their Biotechnological Applications; grant agreement number 311975) to WRH.

References

Allahverdiyeva Y, Ermakova M, Eisenhut M, Zhang P, Richaud P, Hagemann M *et al.* (2011). Interplay between flavodiiron proteins and photorespiration in *Synechocystis* sp. PCC 6803. *J Biol Chem* **286**: 24007–24014.

Allahverdiyeva Y, Mustila H, Ermakova M, Bersanini L, Richaud P, Ajlani G *et al.* (2013). Flavodiiron proteins Flv1 and Flv3 enable cyanobacterial growth and photosynthesis under fluctuating light. *Proc Natl Acad Sci USA* **110**: 4111–4116.

Arambula D, Wong W, Medhekar BA, Guo H, Gingery M, Czornyj E *et al.* (2013). Surface display of a massively variable lipoprotein by a *Legionella* diversity-generating retroelement. *Proc Natl Acad Sci USA* **110**: 8212–8217.

Arnon DI. (1949). Copper enzymes in isolated chloroplasts, polyphenoloxidase in *Beta vulgaris*. *Plant Physiol* **24**: 1–15.

Berghoff BA, Glaeser J, Sharma CM, Vogel J, Klug G. (2009). Photooxidative stress-induced and abundant small RNAs in *Rhodobacter sphaeroides*. *Mol Microbiol* **74**: 1497–1512.

Eisenhut M, Ruth W, Haimovich M, Bauwe H, Kaplan A, Hagemann M. (2008). The photorespiratory glycolate metabolism is essential for cyanobacteria and might have been conveyed endosymbiontically to plants. *Proc Natl Acad Sci USA* **105**: 17199–17204.

Engelken J, Funk C, Adamska I. (2012). The extended light-harvesting complex (LHC) protein superfamily: cassification and evolutionary dynamics. In Burnap RL, Vermaas WFJ (eds). *Functional Genomics and Evolution of Photosynthetic Systems*. Springer: Dordrecht, The Netherlands, pp 265–284.

Fewer DP, Jokela J, Paukku E, Österholm J, Wahlsten M, Permi P *et al.* (2013). New structural variants of aeruginosin produced by the toxic bloom forming cyanobacterium *Nodularia spumigena*. *PLoS One* **8**: e73618.

Funk C, Vermaas W. (1999). A cyanobacterial gene family coding for single-helix proteins resembling part of the light-harvesting proteins from higher plants. *Biochemistry* **38**: 9397–9404.

Garczarek L, Dufresne A, Blot N, Cockshutt AM, Peyrat A, Campbell DA *et al.* (2008). Function and evolution of the psbA gene family in marine *Synechococcus*: *Synechococcus* sp. WH7803 as a case study. *ISME J* **2**: 937–953.

Gehringer MM, Wannicke N. (2014). Climate change and regulation of hepatotoxin production in cyanobacteria. *FEMS Microbiol Ecol* **88**: 1–25.

Georg J, Dienst D, Schürgers N, Wallner T, Kopp D, Stazic D *et al.* (2014). The small regulatory RNA SyR1/PsrR1 controls photosynthetic functions in cyanobacteria. *Plant Cell* **26**: 3661–3679.

Hackenberg C, Engelhardt A, Matthijs HC, Wittink F, Bauwe H, Kaplan A *et al.* (2009). Photorespiratory 2-phosphoglycolate metabolism and photoreduction of O2 cooperate in high-light acclimation of *Synechocystis* sp. strain PCC 6803. *Planta* **230**: 625–637.

Hagemann M, Vinnemeier J, Oberpichler I, Boldt R, Bauwe H. (2005). The glycine decarboxylase complex is not essential for the cyanobacterium *Synechocystis* sp. strain PCC 6803. *Plant Biol* **7**: 15–22.

Hayes PK, Barker GLA. (1997). Genetic diversity within Baltic Sea populations of *Nodularia* (Cyanobacteria). *J Phycol* **33**: 919–923.

He Q, Dolganov N, Bjorkman O, Grossman AR. (2001). The high light-inducible polypeptides in *Synechocystis* PCC6803. Expression and function in high light. *J Biol Chem* **276**: 306–314.

Hernandez-Prieto MA, Futschik ME. (2012). CyanoEXpress: a web database for exploration and visualisation of the integrated transcriptome of cyanobacterium *Synechocystis* sp. PCC6803. *Bioinformation* **8**: 634–638.

Hihara Y, Kamei A, Kanehisa M, Kaplan A, Ikeuchi M. (2001). DNA microarray analysis of cyanobacterial gene expression during acclimation to high light. *Plant Cell* **13**: 793–806.

Kirilovsky D, Kerfeld CA. (2012). The orange carotenoid protein in photoprotection of photosystem II in cyanobacteria. *Biochim Biophys Acta* **1817**: 158–166.

Kopf M, Klähn S, Scholz I, Matthiessen JK, Hess WR, Voß B. (2014). Comparative analysis of the primary transcriptome of *Synechocystis* sp. PCC 6803. *DNA Res* **21**: 527–539.

Los DA, Suzuki I, Zinchenko VV, Murata N. (2008). Stress responses in *Synechocystis*: regulated genes and regulatory systems. In Herrero A, Flores E (eds).

The Cyanobacteria - Molecular Biology, Genomics and Evolution. Caister Academic Press: Norfolk, UK, pp 117–158.

Ludwig M, Bryant DA. (2012). Synechococcus sp. strain PCC 7002 transcriptome: acclimation to temperature, salinity, oxidative stress, and mixotrophic growth conditions. *Front Microbiol* **3**: 354.

Mazur-Marzec H, Kaczkowska MJ, Blaszczyk A, Akcaalan R, Spoof L, Meriluoto J. (2013). Diversity of peptides produced by *Nodularia spumigena* from various geographical regions. *Mar Drugs* **11**: 1–19.

Meissner S, Steinhauser D, Dittmann E. (2014). Metabolomic analysis indicates a pivotal role of the hepatotoxin microcystin in high light adaptation of Microcystis. *Environ Microbiol;* e-pub ahead of print 15 July 2014; doi:10.1111/1462-2920.12565.

Mitschke J, Georg J, Scholz I, Sharma CM, Dienst D, Bantscheff J *et al.* (2011a). An experimentally anchored map of transcriptional start sites in the model cyanobacterium *Synechocystis* sp. PCC6803. *Proc Natl Acad Sci USA* **108**: 2124–2129.

Mitschke J, Vioque A, Haas F, Hess WR, Muro-Pastor AM. (2011b). Dynamics of transcriptional start site selection during nitrogen stress-induced cell differentiation in *Anabaena* sp. PCC7120. *Proc Natl Acad Sci USA* **108**: 20130–20135.

Moffitt MC, Neilan BA. (2004). Characterization of the nodularin synthetase gene cluster and proposed theory of the evolution of cyanobacterial hepatotoxins. *Appl Environ Microbiol* **70**: 6353–6362.

Möke F, Wasmund N, Bauwe H, Hagemann M. (2013). Salt acclimation of *Nodularia spumigena* CCY9414 - a cyanobacterium adapted to brackish water. *Aquat Microb Ecol* **70**: 207–214.

Mulo P, Sakurai I, Aro EM. (2012). Strategies for psbA gene expression in cyanobacteria, green algae and higher plants: from transcription to PSII repair. *Biochim Biophys Acta* **1817**: 247–257.

Paerl HW, Huisman J. (2008). Blooms like it hot. *Science* **320**: 57–58.

Paz-Yepes J, Brahamsha B, Palenik B. (2013). Role of a microcin-C-like biosynthetic gene cluster in allelopathic interactions in marine *Synechococcus*. *Proc Natl Acad Sci USA* **110**: 12030–12035.

Pearson L, Mihali T, Moffitt M, Kellmann R, Neilan B. (2010). On the chemistry, toxicology and genetics of the cyanobacterial toxins, microcystin, nodularin, saxitoxin and cylindrospermopsin. *Mar Drugs* **8**: 1650–1680.

Pfreundt U, Kopf M, Belkin N, Berman-Frank I, Hess WR. (2014). The primary transcriptome of the major marine diazotroph *Trichodesmium erythraeum*. *Sci Rep* **4**: 6187.

Ploug H, Adam B, Musat N, Kalvelage T, Lavik G, Wolf-Gladrow D *et al.* (2011). Carbon, nitrogen and O2 fluxes associated with the cyanobacterium *Nodularia spumigena* in the Baltic Sea. *ISME J* **5**: 1549–1558.

Rippka R, Deruelles J, Waterbury JB, Herdmann M, Stanier RY. (1979). Generic assignments, strain histories and properties of pure cultures of cyanobacteria. *J Gen Microbiol* **111**: 1–61.

Sakurai I, Stazic D, Eisenhut M, Vuorio E, Steglich C, Hess WR *et al.* (2012). Positive regulation of psbA gene expression by cis-encoded antisense RNAs in *Synechocystis* sp. PCC 6803. *Plant Physiol* **160**: 1000–1010.

Scanlan DJ, Ostrowski M, Mazard S, Dufresne A, Garczarek L, Hess WR *et al.* (2009). Ecological genomics of marine picocyanobacteria. *Microbiol Mol Biol Rev* **73**: 249–299.

Sellner KG.. (1997). Physiology, ecology, and toxic properties of marine cyanobacteria blooms. *Limnol Oceanogr* **42**: 1089–1104.

Sharma CM, Hoffmann S, Darfeuille F, Reignier J, Findeiss S, Sittka A *et al.* (2010). The primary transcriptome of the major human pathogen *Helicobacter pylori*. *Nature* **464**: 250–255.

Sicora CI, Ho FM, Salminen T, Styring S, Aro EM. (2009). Transcription of a ''silent'' cyanobacterial psbA gene is induced by microaerobic conditions. *Biochim Biophys Acta* **1787**: 105–112.

Sivonen K, Halinen K, Sihvonen LM, Koskenniemi K, Sinkko H, Rantasärkkä K *et al.* (2007). Bacterial diversity and function in the Baltic Sea with an emphasis on cyanobacteria. *Ambio* **36**: 180–185.

Summerfield TC, Toepel J, Sherman LA. (2008). Low-oxygen induction of normally cryptic psbA genes in cyanobacteria. *Biochemistry* **47**: 12939–12941.

Voß B, Bolhuis H, Fewer DP, Kopf M, Möke F, Haas F *et al.* (2013). Insights into the physiology and ecology of the brackish-water-adapted cyanobacterium *Nodularia spumigena* CCY9414 based on a genome-transcriptome analysis. *PLoS One* **8**: e60224.

Wu Z, Jenkins BD, Rynearson TA, Dyhrman ST, Saito MA, Mercier M *et al.* (2010). Empirical bayes analysis of sequencing-based transcriptional profiling without replicates. *BMC Bioinform* **11**: 564.

Xu H, Vavilin D, Funk C, Vermaas W. (2004). Multiple deletions of small Cab-like proteins in the cyanobacterium *Synechocystis* sp. PCC 6803: consequences for pigment biosynthesis and accumulation. *J Biol Chem* **279**: 27971–27979.

Yoshida-Takashima Y, Yoshida M, Ogata H, Nagasaki K, Hiroishi S, Yoshida T. (2012). Cyanophage infection in the bloom-forming cyanobacteria *Microcystis aeruginosa* in surface freshwater. *Microbes Environ* **27**: 350–355.

Zehr JP. (2011). Nitrogen fixation by marine cyanobacteria. *Trends Microbiol* **19**: 162–173.

Zilliges Y, Kehr JC, Meissner S, Ishida K, Mikkat S, Hagemann M *et al.* (2011). The cyanobacterial hepatotoxin microcystin binds to proteins and increases the fitness of microcystis under oxidative stress conditions. *PLoS One* **18**: e17615.

Supplementary Information accompanies this paper on The ISME Journal website (http://www.nature.com/ismej)